The Journal of Experimental Medicine

Transglutaminase is essential for IgA nephropathy development acting through IgA receptors

Laureline Berthelot,[1,2] Christina Papista,[1,2] Thiago T. Maciel,[1,2] Martine Biarnes-Pelicot,[1,2] Emilie Tissandie,[1,2] Pamela H.M. Wang,[1,2] Houda Tamouza,[1,2] Agnès Jamin,[1,2] Julie Bex-Coudrat,[1,2] Aurelie Gestin,[1,2] Ahmed Boumediene,[3] Michelle Arcos-Fajardo,[1,2] Patrick England,[4] Evangéline Pillebout,[1,2,5] Francine Walker,[6] Eric Daugas,[1,2,7] François Vrtovsnik,[1,2,7] Martin Flamant,[1,2,8] Marc Benhamou,[1,2] Michel Cogné,[3] Ivan C. Moura,[1,2] and Renato C. Monteiro[1,2,9]

[1]Institut National de la Santé et de la Recherche Médicale Unité Mixte de Recherche 699, Paris 75870, France
[2]Laboratoire d'Excellence Inflamex, Faculté de Médecine, Site Xavier Bichat, Université Paris Diderot, Sorbonne Paris Cité, Paris 75018, France
[3]Centre National de la Recherche Scientifique Unité Mixte de Recherche 6101, Université de Limoges, Limoges 87000, France
[4]Proteopole, Institut Pasteur, Paris 75015, France
[5]Service de Néphrologie, Hôpital Saint-Louis, Paris 75010, France
[6]Service d'Anatomo-Pathologie, [7]Service de Néphrologie, [8]Service de Physiologie et Explorations Fonctionnelles Multidisciplinaire, and [9]Service d'Immunologie, Assistance Publique de Paris, Hôpital Bichat-Claude Bernard, Paris 75870, France

IgA nephropathy (IgAN) is a common cause of renal failure worldwide. Treatment is limited because of a complex pathogenesis, including unknown factors favoring IgA1 deposition in the glomerular mesangium. IgA receptor abnormalities are implicated, including circulating IgA–soluble CD89 (sCD89) complexes and overexpression of the mesangial IgA1 receptor, TfR1 (transferrin receptor 1). Herein, we show that although mice expressing both human IgA1 and CD89 displayed circulating and mesangial deposits of IgA1–sCD89 complexes resulting in kidney inflammation, hematuria, and proteinuria, mice expressing IgA1 only displayed endocapillary IgA1 deposition but neither mesangial injury nor kidney dysfunction. sCD89 injection into IgA1-expressing mouse recipients induced mesangial IgA1 deposits. sCD89 was also detected in patient and mouse mesangium. IgA1 deposition involved a direct binding of sCD89 to mesangial TfR1 resulting in TfR1 up-regulation. sCD89–TfR1 inter-action induced mesangial surface expression of TGase2 (transglutaminase 2), which in turn up-regulated TfR1 expression. In the absence of TGase2, IgA1–sCD89 deposits were dra-matically impaired. These data reveal a cooperation between IgA1, sCD89, TfR1, and TGase2 on mesangial cells needed for disease development. They demonstrate that TGase2 is responsible for a pathogenic amplification loop facilitating IgA1–sCD89 deposition and mesangial cell activation, thus identifying TGase2 as a target for therapeutic intervention in this disease.

IgA nephropathy (IgAN), a major cause of end-stage renal disease (Donadio and Grande, 2002), affects both native and transplanted kidneys with recurrence after transplantation occurring in about one third of patients (Berger et al., 1975; Ponticelli and Glassock, 2010). Mesangial IgA deposits, mainly characterized as of the IgA1 subclass, appear as the first step of the disease together with circulating immune complexes containing IgA1 with abnormal O-linked glycosylation

(Monteiro et al., 1985; Tomana et al., 1999; Novak et al., 2008; Tissandié et al., 2011). IgAs are unique immunoglobulins with exceptional heterogeneity. In addition to secreted and serum forms, they exist as two subclasses (IgA1 and IgA2) and are present in the circulation as monomers and polymers that are covalently associated by

the joining (J) chain. In healthy individuals (contrary to other species like the mouse), circulating IgAs are essentially monomeric. IgA receptors (IgARs) have been proposed to play a role in IgAN pathogenesis (Monteiro et al., 2002). Within the family of multiple IgARs, the myeloid FcαRI (CD89) and TfR1 (transferrin receptor 1; CD71) were identified as putative pathogenic factors in IgAN patients with altered expression on monocytes (Grossetête et al., 1998) and mesangial cells (Moura et al., 2001), respectively. Although CD89 shedding from myeloid cells results in pathogenic soluble forms complexed to IgA (Launay et al., 2000), TfR1 is overexpressed on mesangial cells after IgA1 complex deposition (Haddad et al., 2003). Deposits of IgA1 immune complexes in the mesangium could thus be formed through interaction of these complexes with the mesangial TfR1, but this could not be experimentally demonstrated in vivo because of the lack of a valid animal model reproducing the human IgA1 system. Previously, we have shown that transgenic (Tg) mice expressing the human CD89 on monocytes/macrophages display mouse IgA–human CD89 interaction on these cells and spontaneously develop mouse IgA deposits in their mesangium at 24 wk (Launay et al., 2000). However, it has been claimed that mouse IgAs fail to bind to human CD89 in vitro (Pleass et al., 1999) and that injection of soluble CD89 (sCD89) does not induce mouse IgA deposition in the mesangium (van der Boog et al., 2004). The role of mouse IgA–human sCD89 complexes in IgAN development in CD89Tg mice was indirectly demonstrated by serum transfer experiments from CD89Tg into RAG-2$^{-/-}$ mice or from IgAN patients into NOD.SCID mice, leading to disease development, which was lost by anti-CD89 immunoabsorption (Launay et al., 2000). More recently, patients with severe IgAN were shown to present decreased levels of IgA–sCD89 complexes in the circulation (Vuong et al., 2010). Whether sCD89 plays a deleterious or protective role in IgAN pathogenesis is a question that has been raised recently (Boyd and Barratt, 2010). sCD89's role in mesangial IgA1 deposit formation and disease progression remains thus elusive and could involve TfR1 and other unknown molecular partners.

To elucidate the role of CD89 in the pathogenesis of the disease, we have generated Tg mice expressing both human IgA1 (Duchez et al., 2010) and human CD89 (α1KI-CD89Tg mice). Extensive mesangial deposits of IgA1 and sCD89 appeared at 12 wk in α1KI-CD89Tg mice associated with C3 and mannan–binding lectin (MBL) deposits, as well as increased macrophage infiltration, proteinuria, hematuria, and serum creatine levels. Kidney biopsies from IgAN patients were also positively stained for sCD89. Injection of sCD89 in α1KI mice induced TfR1 overexpression and IgA1 mesangial deposition. sCD89 directly interacted with sTfR1 in vitro and stimulated mesangial cells for production of inflammatory cytokines IL-8, IL-6, and TNF. CD89 expression in α1KI mice also resulted in mesangial overexpression of TGase2 (transglutaminase 2), which colocalized with IgA1. In vitro, sCD89 induced TGase2 surface expression on mesangial cells. TGase2 also bound to TfR1, inducing its overexpression and facilitating

IgA1 binding on mesangial cells, whereas no disease was induced in TGase2-deficient animals. Therefore, our observations in a humanized mouse model for the IgA1 system as well as in humans document the importance of sCD89 in the induction of the mesangial IgA1 receptor TfR1 expression and in the development of IgAN and support a model that, besides IgA1, sCD89, and TfR1, involves TGase2 as a key player in the complex pathogenic mechanism of this disease.

RESULTS
Mice expressing human IgA1 and CD89 developed early mesangial IgA1 deposits with hematuria and overt proteinuria

The IgA system differs between humans and mice (Kerr, 1990). Although humans display two IgA subclasses and a myeloid IgAR belonging to the Fc receptor family, the CD89 (or FcαRI), mice have only one IgA subclass differing from the human counterpart by its shorter hinge region (where O-glycosylation occurs) and lack a CD89 homologue (Monteiro and Van De Winkel, 2003). Therefore, to establish a model that mimics human IgAN, we backcrossed CD89Tg mice with α1KI mice, which produce significant amounts of human IgA1 in the circulation (0.5–1 mg/ml; Duchez et al., 2010). Although both α1KI and α1KI-CD89Tg mice presented glomerular deposits of IgA1 at 12 wk of age, α1KI-CD89Tg mice displayed typical mesangial IgA1 deposits, whereas α1KI mice exhibited diffuse endocapillary deposits of IgA1 (Fig. 1 A). The latter was demonstrated by confocal immunofluorescence analysis showing extensive colocalization of the vascular marker CD31 with IgA1 deposits within the capillary walls of α1KI but not α1KI-CD89Tg mice (Fig. 1 A). Moreover, dense materials were observed in the mesangial area for α1KI-CD89Tg mice and in the endocapillary area for α1KI mice using transmission electron microscopy (Fig. 1 B). Mesangial IgA1 deposits started at 6 wk of age in α1KI-CD89Tg mice with an intense pattern detected starting at 12 wk (Fig. 1 C). This contrasted with the late detection of mouse IgA staining observed in 24–wk-old CD89Tg mice in similar 129-C57BL/6 background, confirming our previous observations in NOD.C57BL/6 CD89Tg mice (not depicted; Launay et al., 2000). To address whether these differences in IgA1 deposition kinetics resulted from affinity differences between mouse and human IgA to CD89, we performed surface plasmon resonance experiments using recombinant sCD89. Mouse IgA interacted with sCD89 with a very low affinity (K$_D$ ∼7.6 × 10^{-5} M; Fig. 1 D), which was 100 times lower than that of human IgA1 and of monoclonal human IgA1 obtained from α1KI mice (Fig. 1 E). Moreover, morphological analyses of α1KI-CD89Tg kidneys showed expansion of mesangial extra cellular matrix as indicated by periodic acid Schiff (PAS) staining (Fig. 1 A), which was also accompanied by fibronectin overexpression (Fig. 1 A).

α1KI-CD89Tg mice exhibited marked MBL and C3 glomerular deposits, hallmarks of IgAN, whereas in α1KI and WT mice, these deposits were notably less intense (Fig. 2 A). As anti-IgA1 IgG have been reported in patients (Suzuki et al., 2009),
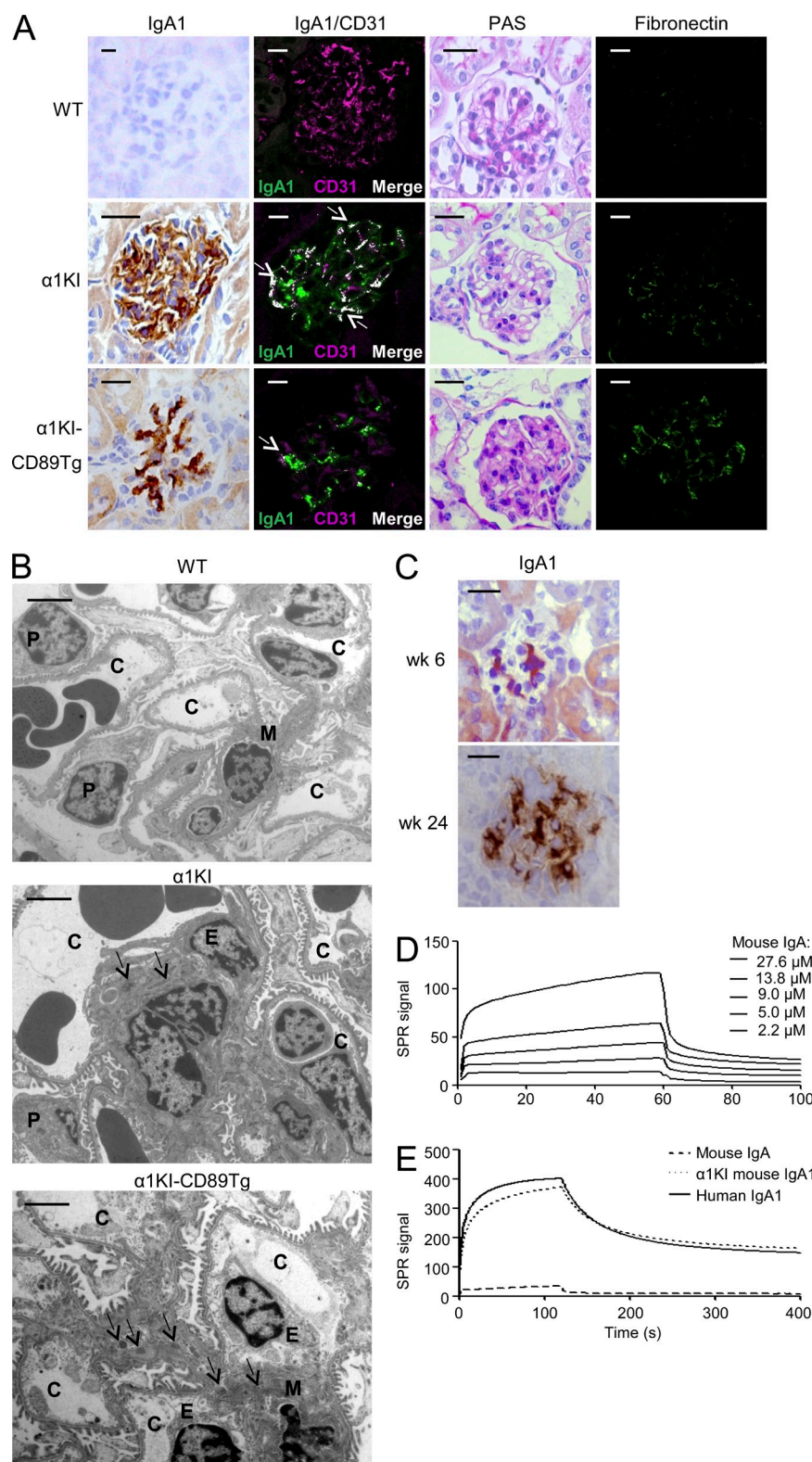
Figure 1. CD89 determines mesangial deposition of IgA1. (A) From left to right: immunostaining for human IgA1 in frozen kidney sections, double immunofluorescence for human IgA1 and CD31, PAS staining of paraffin-embedded kidney sections, and immunofluorescent staining for fibronectin in frozen sections from α1KI-CD89Tg versus α1KI and WT mice (12 wk old). Arrows indicate colocalization of IgA1 and CD31. (B) Transmission electron microscopy pictomicrographs of glomeruli from α1KI-CD89Tg versus α1KI and WT mice (12 wk old). C, capillary; E, endothelial cell; M, mesangial cell; P, podocyte. Arrows indicate dense materials. (C) Immunostaining for human IgA1 in frozen kidney sections of 6- and 24-wk-old α1KI-CD89Tg mice. Bars: (A and C) 10 μm; (B) 2 μm. (D) Dose-dependent interaction of mouse IgA with sCD89 monitored by real-time surface plasmon resonance (SPR).(E) Association of different types of IgA (mouse IgA, α1KI mouse IgA1, and human IgA1; 5 μM) with sCD89.

was significantly observed in glomeruli and periglomerular interstitial areas of α1KI-CD89Tg mice, indicating that a local inflammation occurs in kidneys of these mice that express human CD89. α1KI-CD89Tg mice also presented features of altered kidney function such as proteinuria, albuminuria, hematuria, and increase in serum creatinine levels (Fig. 2, C–G). Proteinuria started at 12 wk and was more intense at 24 wk (Fig. 2 D). Although no significant proteinuria was found in α1KI mice, CD89Tg mice in the 129-C57BL/6 background displayed very mild proteinuria (not depicted) as previously described (Launay et al., 2000). However, proteinuria was completely abolished in NOD.SCID-CD89Tg mice that lack IgA (not depicted). Collectively, these results show that the presence of both human IgA1 and CD89 promotes increased mesangial IgA1 deposition, hematuria and proteinuria, and altered renal function in mice.

sCD89 induces high molecular mass circulating IgA1 complexes and mediates mesangial IgA1 deposition

As α1KI-CD89Tg mice developed pathogenic mesangial IgA1 deposits, we next investigated whether circulating sCD89 was complexed with IgA1. Cell surface expression of CD89 on blood monocytes,

we assessed the presence of IgG in mouse kidneys using an anti-IgG antibody. There was no detectable deposition of IgG in α1KI and α1KI-CD89Tg kidneys (not depicted). Marked infiltration of CD11b+ (Fig. 2 B) and F4/80+ (not depicted) cells

absent in α1KI and WT mice, was lower in α1KI-CD89Tg than in CD89Tg mice (Fig. 3 A), suggesting that expression of human IgA1 in mice may enhance shedding of CD89 as previously shown in vitro (Launay et al., 2000). Similar results

were obtained with splenic macrophages (not depicted). sCD89 was found complexed with IgA1 (Fig. 3 B), and no free sCD89 (not depicted) was detected in the serum of α1KI-CD89Tg mice using two mAbs, anti-CD89 A3 and MIP8a, an mAb that recognizes CD89 IgA binding site (Zhang et al., 2000). Similar data were observed in IgAN patient sera (Fig. 3 C), confirming our previous observations (Launay et al., 2000). Despite the fact that α1KI and α1KI-CD89Tg mice presented similar levels of IgA1 in their sera (Fig. 3 D), only α1KI-CD89Tg mice exhibited large molecular mass IgA1 complexes (>670 kD) in the serum as detected by Western blotting and HPLC analysis (Fig. 3, E and G), whereas α1KI displayed essentially monomers and dimers (Fig. 3, E and F). IgA1–sCD89 complexes were detected by ELISA in size-fractionated serum (fractions 6–9), corresponding to high mass molecular forms (Fig. 3 G).

The presence of sCD89 was further demonstrated in fractions containing high molecular mass IgA1 complexes by immunoprecipitation assays using anti-CD89 mAb A3 coupled to beads followed by SDS-PAGE at nonreducing conditions and Western blotting using a cocktail of anti-CD89 mAbs (Fig. 3 H). A 50–70-kD sCD89 protein was detected under reducing conditions overlapping the α chain (not depicted) as previously described (Launay et al., 2000).

We next assessed the presence of CD89 in the mesangium by using an anti-sCD89 polyclonal antibody. α1KI-CD89Tg kidney sections displayed positive stainings for CD89 with a typical mesangial pattern (Fig. 4 A). We then addressed whether anti-sCD89 polyclonal antibody stained CD89 on biopsies from IgAN patients. As shown in Fig. 4 B, a mesangial pattern of CD89 staining was observed that was abolished in the presence of an excess of sCD89. This staining was confirmed in biopsies from two additional IgAN patients but not in biopsies from patients with minimal change disease (not depicted). To formally demonstrate that sCD89 is responsible for mesangial IgA1 deposition, we injected recombinant sCD89 into 6-wk-old α1KI mice because they display very few deposits of IgA1 in their glomerular capillary walls. sCD89 induced massive mesangial IgA1 deposits when compared with mice that received an irrelevant control protein BSA (Fig. 4 C).
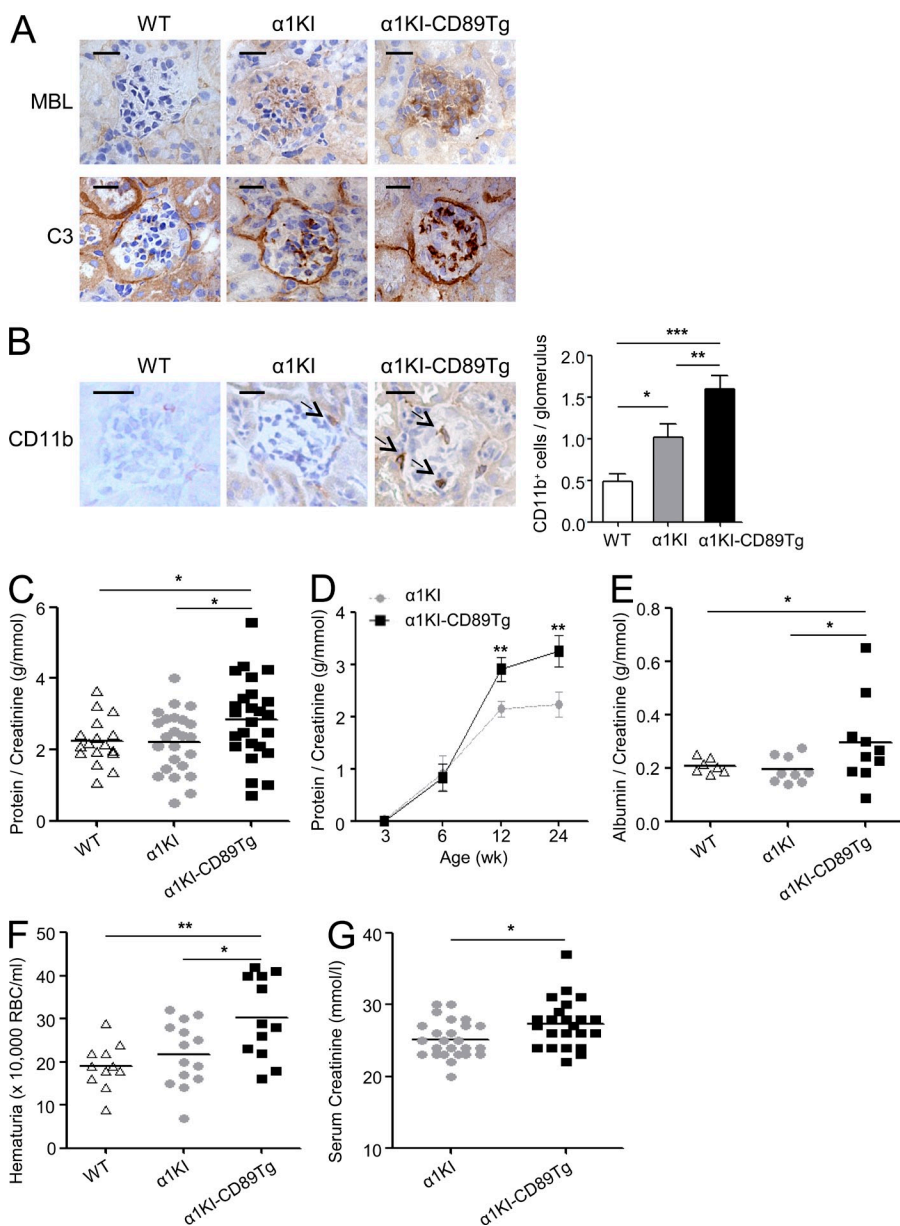

Figure 2. CD89 is required for complement deposition, leukocyte infiltration, proteinuria, and hematuria. (A) Deposits of MBL and C3 detected by immunohistochemistry in frozen kidney sections of 12-wk-old α1KI-CD89Tg compared with α1KI and WT mice. (B) Immunostaining for the detection of CD11b+ infiltrates in frozen kidney sections of mice. (left) Representative sections. Arrows indicate CD11b+ cells. (right) Numbers of positive cells per glomerulus counted in 20 randomly chosen fields for each mouse at 200 magnification. n = 4 mice per group. Bars, 10 µm. (C and D) Protein to creatinine ratio measured in the urines of 12-wk-old α1KI-CD89Tg mice compared with WT and α1KI (C) and 3-, 6-, 12-, and 24-wk-old α1KI and α1KI-CD89Tg mice (D). 7–20 mice per group. (B and D) Error bars indicate SEM. (E and F) Ratio of albumin to creatinine (E) and hematuria (×10,000 red cells/ml; F) as measured in the urines of 12-wk-old WT, α1KI, and α1KI-CD89Tg mice. 7–14 mice per group. (G) Levels of creatinine in the serum of 12-wk-old α1KI and α1KI-CD89Tg mice. 23–25 mice per group. Bars represent the mean. *, P < 0.05; **, P < 0.01; and ***, P < 0.001 (using the nonparametric Mann-Whitney U test).
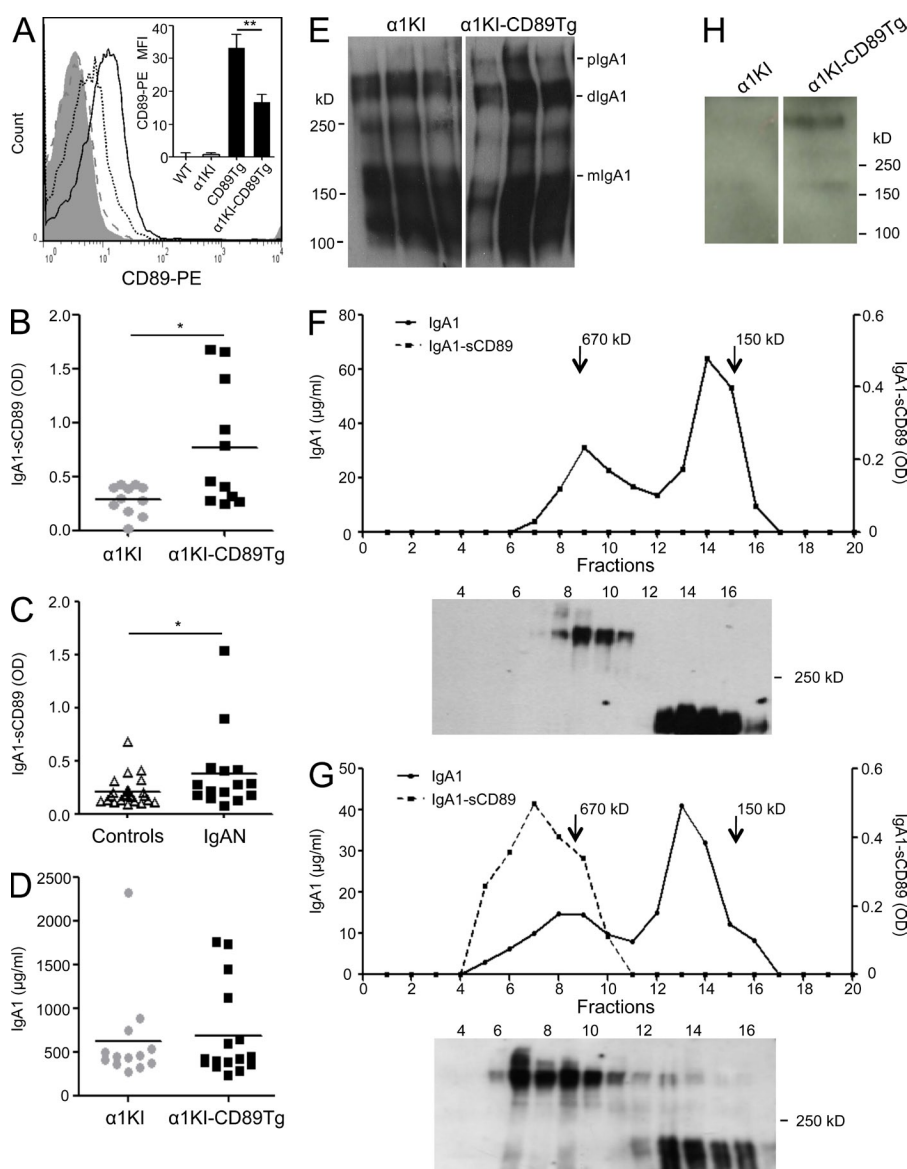
To further determine the nature of CD89 (soluble or trans-membrane form ectopically expressed on infiltrating cells) deposited in mesangial areas of α1KI-CD89Tg mice, saline-perfused kidneys were subjected to acid elution procedures as described previously (Monteiro et al., 1985). After neutralization, IgA1–sCD89 complexes were detected by ELISA in eluates from α1KI-CD89Tg mice but not in those from α1KI mice (Fig. 4 D). More importantly, size exclusion resolution of kidney eluates revealed that high molecular mass IgA1 complexes (>670 kD) represented the predominant form (56%) of IgA1 present in mesangial deposits of α1KI-CD89Tg mice (Fig. 4 E), confirming data previously observed in IgAN patients and further demonstrating that macromolecular IgA is the main IgA form trapped in mesangial areas (Monteiro et al., 1985). As observed previously with CD89Tg mice (Launay et al., 2000), the ability of IgA1–sCD89 complexes to transfer the disease was demonstrated in NOD.SCID mice that developed

IgA1 mesangial deposits and hematuria 24 h after injection of serum from α1KI-CD89Tg mice (not depicted). Together, α1KI-CD89Tg mice data indicated that circulating high molecular mass IgA1–sCD89 complexes are responsible for mesangial IgA1 deposition in IgAN.

sCD89 binds to TfR1 and induces its overexpression on mesangial cells

TfR1 is an IgA1 receptor that is overexpressed in the mesangium of patients with IgAN (Moura et al., 2001; Haddad et al., 2003) and enterocytes from patients with celiac disease (Matysiak-Budnik et al., 2008). As human IgA1 interacts with mouse TfR1 (Coulon et al., 2011), we next examined whether knockin expression of human IgA1 in the mouse could induce mesangial TfR1 expression and whether this overexpression was dependent on CD89. Although α1KI mice displayed a slight increase in TfR1+ cells in their mesangium, the presence of CD89 markedly enhanced (more than threefold) the TfR1 expression in the mesangium of α1KI-CD89Tg mice (Fig. 5 A). CD89-mediated overexpression of TfR1 increased with age

Figure 3. sCD89 induces high molecular mass circulating IgA1 complex formation. (A) Surface staining of CD89 on mouse blood monocytes. The white layer represents CD89Tg, dotted for α1KI-CD89Tg, dashed for α1KI, and gray for WT cells. The graph shows the mean fluorescent intensity (MFI) of CD89 on CD11b+ cells. 5–30 mice per group. Error bars show mean ± SEM. (B and C) Detection of IgA1–sCD89 complexes in the sera of mice (B) and patients (C) by ELISA. For detection of these complexes, A3 anti-CD89 was used as a coating antibody and monoclonal anti–human IgA as a secondary reagent. n = 11 mice per group and 15–25 individuals per group. Bars represent the mean of OD. (D) IgA1 levels in the serum of 12-wk-old α1KI and α1KI-CD89Tg mice measured by ELISA. 11–16 mice per group. Bars represent the mean. (E) Immunoblot of monomeric (m), dimeric (d), and polymeric (p) forms of IgA1 in sera (normalized at 0.1 µg IgA1 per sample) from α1KI and α1KI-CD89Tg mice with an anti–human IgA polyclonal antibody. (F and G) Total IgA detected by ELISA and Western blot in serum HPLC fractions of one representative α1KI (F) and one α1KI-CD89Tg mouse (G). n = 3 mice per group. Detection of IgA1–sCD89 complexes in these fractions by ELISA shows that they correspond to high molecular mass IgA1 fractions. (H) Immunoblot on material immunoprecipitated from anti-CD89 serum from α1KI and α1KI-CD89Tg mice using a mixture of anti-CD89 mAbs. *, P < 0.05; and **, P < 0.01 (Mann-Whitney U test).

(not depicted). Moreover, injections of recombinant sCD89 in 6-wk-old α1KI mice, which markedly increased IgA1 deposits (see Fig. 4 C), induced TfR1 overexpression in the mesangium (Fig. 5 B). In addition, TfR1 was overexpressed in the kidneys of immunodeficient NOD.SCID mice that received recombinant sCD89 alone, whereas BSA had no effect (Fig. 5 C).

To elucidate the mechanism by which the presence of sCD89 in mice induces TfR1 overexpression on mesangial cells, we first assessed whether sCD89 alone could bind to human mesangial cells (HMCs) in the absence of IgA. sCD89 bound to HMCs in a dose-dependent manner (Fig. 5 D, inset), and this binding was specifically inhibited by recombinant sTfR1

Figure 4. **sCD89 mediates mesangial IgA1 deposition in mice and is detected in glomeruli of patients.** (A) Immunohistochemistry for the detection of CD89 deposits using the rabbit polyclonal anti-sCD89 in α1KI-CD89Tg versus α1KI and WT mice (12 wk old). (B) Detection of CD89 deposits by immunohistochemistry in biopsies of IgAN patients and controls using the rabbit polyclonal antibody pretreated or not with 500 µg/ml sCD89. Arrows indicate sCD89 deposits. (C) Immunostaining for human IgA in frozen kidney sections of 6-wk-old α1KI mice injected i.v. with BSA or sCD89. Bars: (A and C) 10 µm; (B) 20 µm. (D) Detection of IgA1–sCD89 complexes in kidney eluates from α1KI and α1KI-CD89Tg mice by ELISA using a monoclonal anti-CD89 (A3) and a polyclonal anti–human IgA antibody. Error bars indicate SEM. $n = 7$ mice per group. (E) Total IgA detected by ELISA in HPLC fractions of kidney eluates from α1KI-CD89Tg mice.

(53% inhibition; Fig. 5 D). TfR1 microRNA (miRNA) treatment, which down-regulated TfR1 cell membrane expression (50% decrease; Fig. 5 E, inset), resulted also in a decreased binding of sCD89 to HMCs (49% decrease; Fig. 5 E). A direct molecular binding was detected between sCD89 and sTfR1 by ELISA (Fig. 5 F) and by pull-down experiments (Fig. 5 G). To formally demonstrate the role of sCD89 in TfR1 expression, we next stimulated quiescent HMCs in culture with recombinant sCD89 in the absence of IgA. This treatment resulted in TfR1 overexpression on these cells (96% increase) over a 48-h period (Fig. 5 H) with an increase of its messenger RNA (mRNA) levels (Fig. 5 I). All of the aforementioned data demonstrate that sCD89 can directly interact with TfR1 and induce its overexpression on mesangial cells even in the absence of IgA.

To examine whether sCD89 is directly involved in IgA1 binding to HMCs, we incubated these cells on ice with preformed IgA1–sCD89 complexes for 1 h and assessed for IgA binding by flow cytometry using an anti-IgA antibody. sCD89 complexed to IgA1 led to increased IgA1 binding to mesangial cells (Fig. 6 A). To precisely localize the interactions of IgA1–sCD89 complexes on HMCs, we next visualized these interactions in vitro using confocal microscopy. IgA1 and sCD89 were colocalized on the cell surface of HMCs (Fig. 6 B). Therefore, sCD89 plays an essential role in tissue IgA1 deposit formation, both by increasing TfR1 expression and by facilitating IgA1 binding on mesangial cells. To evaluate the functional role of these proteins, we then analyzed the effect of IgA1 or IgA1–sCD89 complexes on the secretion of IL-8, IL-6, and TNF on HMCs in culture. In line with the increased binding of IgA1–sCD89 complexes (Fig. 6 A), these complexes induced strong secretion of IL-6 and IL-8 cytokines as compared with stimulation with IgA1 alone (Fig. 6 C). However, IgA1 alone induced TNF secretion and only marginal IL-8 and IL-6 secretion as compared with sCD89 (Fig. 6 C). TfR1 miRNA treatment of HMCs markedly decreased the ability of IgA1–sCD89 complexes to stimulate cytokine secretion (Fig. 6 D). Because sCD89 was required for mesangial IgA1 deposits, we next explored whether IgA1 and CD89 expression in the mouse had renal functional consequences by analyzing tissue mRNA levels of proinflammatory cytokines using saline-perfused kidneys. α1KI-CD89Tg mice presented a marked increase in mRNA levels for MIP-2, IL-6, and TNF cytokines (Fig. 6 E). Therefore, both IgA1 and sCD89 within the IgA1–sCD89 complexes cooperate to induce mesangial TfR1 expression and kidney inflammation in IgAN.
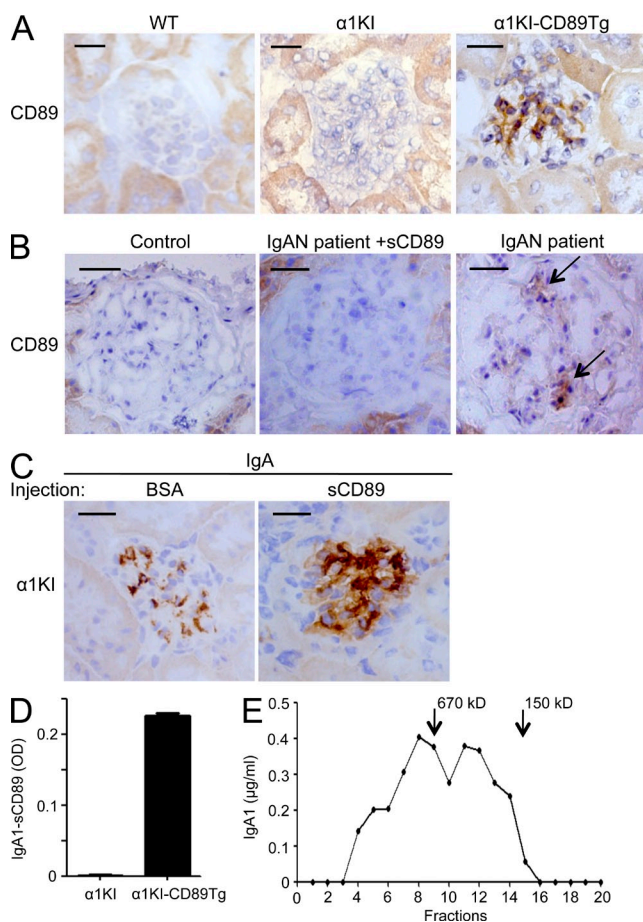
sCD89 induces TGase2 mesangial surface expression, which is associated with TfR1 and is crucial for IgA1 deposit formation

TfR1 is ubiquitously expressed to perform its major function of iron uptake through transferrin (Ganz, 2008). The observation of TfR1 as an IgA1 receptor has been established in pathological settings where TfR1 is overexpressed by tissues, notably by mesangial and epithelial cells (Moura et al., 2001; Matysiak-Budnik et al., 2008). Because IgA1 binding depends on the density of TfR1 expressed on the cell surface (Moura et al., 2004b),
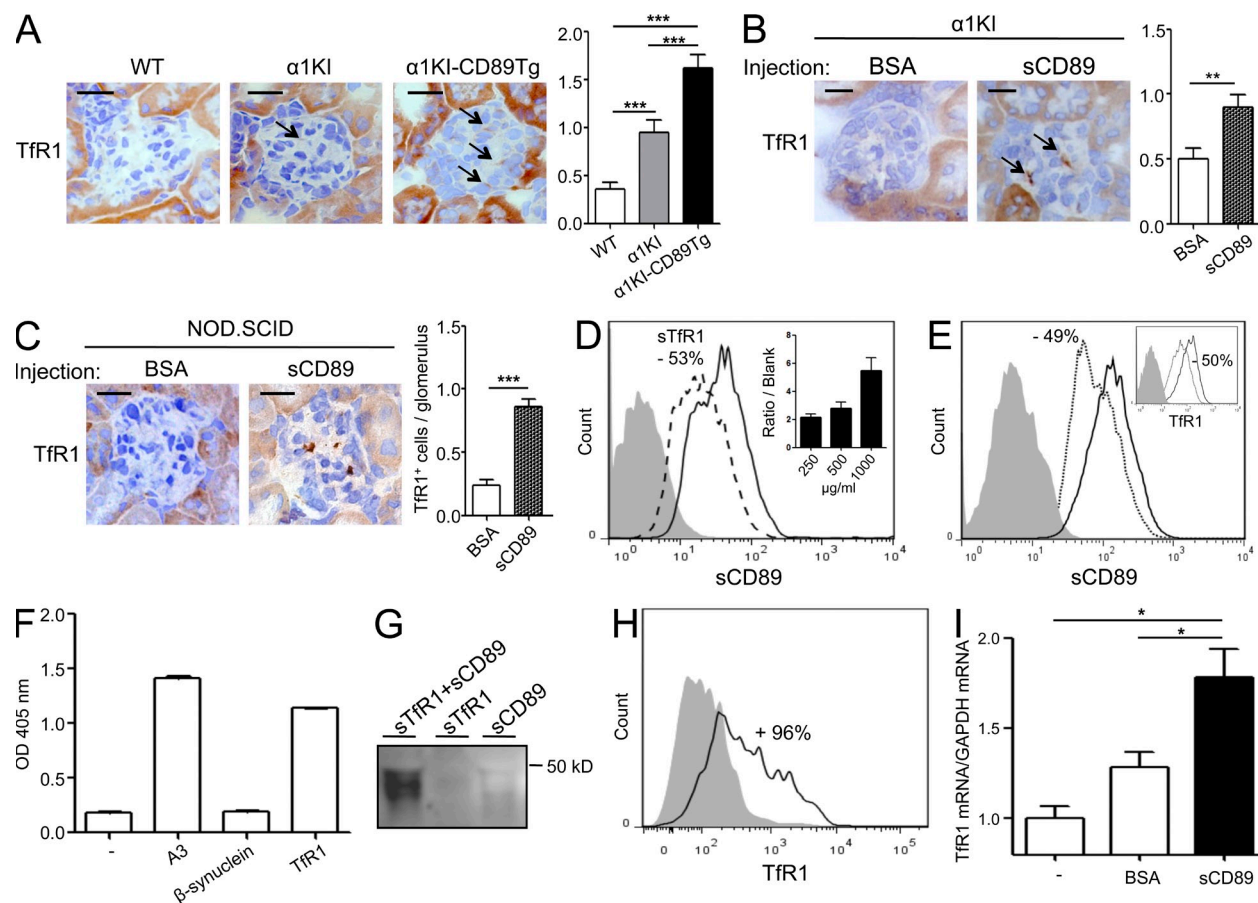
Figure 5. sCD89 interacts with TfR1 and induces up-regulation of its expression on mesangial cells. (A–C) Frozen kidney sections immunostained for mouse TfR1 from 12-wk-old WT, α1KI, and α1KI-CD89Tg mice (A), 6-wk-old α1KI mice injected i.v. with BSA or sCD89 (B), and NOD.SCID mice injected with BSA or sCD89 (C). Arrows indicate TfR1+ cells. The corresponding graphs represent the numbers of positive cells per glomerulus counted in 20 randomly chosen fields for each mouse at 200 magnification. n = 3 mice per group. Bars: (A) 10 µm; (B and C) 5 µm. (D) Flow cytometry histogram (one representative experiment of six) of HMCs binding sCD89 (white layer) and stained with anti-CD89. The dashed layer represents incubation with sTfR1. The gray layer corresponds to the isotypic-matched control. The inset graph shows the mean binding values of indicated doses of sCD89 (±SEM) to HMCs as a ratio to background mean fluorescence intensity of seven independent experiments. (E) Flow cytometry analysis of sCD89 binding on HMCs untreated (white layer) or treated with TfR1 miRNA (dotted layer). The inset shows flow cytometry analysis of TfR1 expression on HMCs untreated (white layer) or treated with TfR1 miRNA (dotted layer). The histogram shows one representative experiment of six. The gray layers correspond to the isotypic-matched controls. (F) Binding of sCD89 to TfR1-His by ELISA using biotinylated sCD89. 10 µg/ml sTfR1 was coated in ELISA plates and incubated with the indicated doses of biotinylated sCD89. β-Synuclein is a His-tagged protein used as a negative control and A3 an anti-CD89 mAb as a positive control. n = 4 experiments. (G) sCD89 interaction with recombinant sTfR1. sCD89 was loaded on a column of nickel beads preincubated or not with sTfR1-His. Eluates were analyzed by SDS–10% PAGE followed by Western blot using a cocktail of anti-CD89 antibodies. (H) Flow cytometry analysis of TfR1 expression on HMCs unstimulated (gray layer) or stimulated with sCD89 (white layer). The histogram shows one representative experiment of six. (I) mRNA levels of TfR1 normalized to GAPDH mRNA levels in HMCs stimulated with sCD89 or BSA. (A–C, F, and I) Error bars indicate SEM. *, P < 0.05 (unpaired Student's t test); **, P < 0.01; and ***, P < 0.001 (Mann-Whitney U test).

we investigated whether tissue mesangial cells express a protein associated to TfR1 that may control the expression of TfR1 and therefore favor IgA1 binding. Because TGase2, a cross-linking enzyme with pleiotropic functions (Lorand and Graham, 2003), is overexpressed in the mesangium of IgAN patients and correlated with renal function decline (Ikee et al., 2007), we examined whether it could modulate IgA1 complex deposition and TfR1 expression. TGase2 expression was markedly up-regulated in the mesangium of α1KI-CD89Tg mice, whereas it was only weakly detected in α1KI and absent in WT mice (Fig. 7 A), indicating a role of sCD89 in its regulation. Mesangial TGase2 over-expression was confirmed in biopsies of IgAN patients (Fig. 7 B),

as reported by others (Ikee et al., 2007). This was also supported by experiments in which injection of recombinant sCD89 in α1KI mice resulted in increased TGase2 staining (Fig. 7 C). Recombinant sCD89 but not IgA1 also up-regulated TGase2 expression on the surface of HMCs (approximately threefold increase; Fig. 7 D). However, IgA1 strongly bound to TGase2 in an antibody-independent manner because normal human serum IgA as well as antiovalbumin IgA1 mAb obtained from hybridoma derived from α1KI mice equally bound to TGase2 (Fig. 8 A) and not mouse IgG (not depicted). Confocal analysis of kidney sections revealed that TGase2 was strongly colocalized with mesangial IgA1 deposits in α1KI-CD89Tg mice but not in
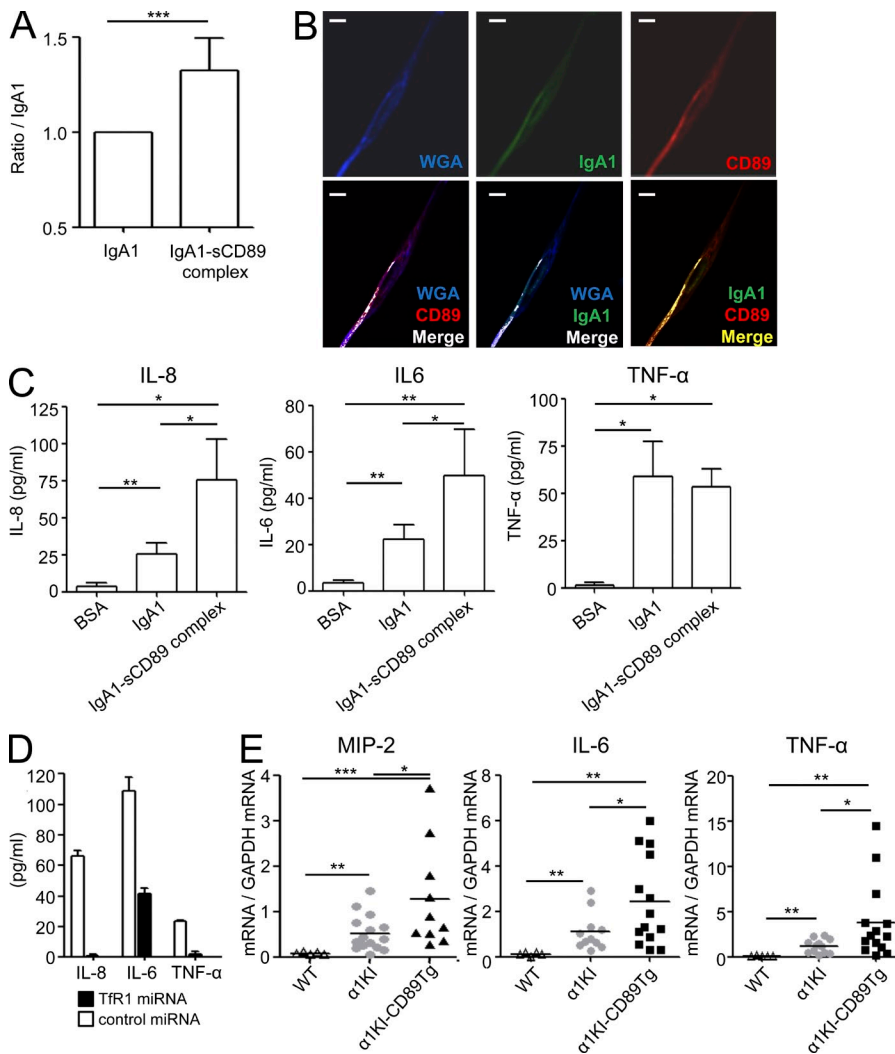
Figure 6. sCD89–TfR1 interaction favors IgA1 deposition and activates mesangial cells. (A) HMCs were incubated with the IgA1 or IgA1–sCD89 complexes at 4°C, and binding was detected using anti–IgA-FITC. The graph shows the mean of IgA1 binding (±SEM) as a mean fluorescence intensity ratio to background of six independent experiments. (B) Cell surface colocalization of IgA1 and CD89 on HMCs after incubation with IgA1–sCD89 complexes on ice. Wheat germ agglutinin (WGA) was used as cell membrane marker. Bars, 2 µm. (C) Detection of IL-8, IL-6, and TNF in the supernatant of HMCs stimulated for 48 h with BSA, IgA1, and IgA1–sCD89 complexes. n = 6 experiments. (D) Cytokine production after stimulation of TfR1 miRNA–treated HMCs with IgA1–sCD89 complexes for 8 h. n = 3 experiments. HMCs were infected with lentivirus bearing either TfR1 miRNA or irrelevant miRNA. (C and D) Error bars indicate SEM. (E) mRNA levels of MIP-2, IL-6, and TNF normalized to GAPDH mRNA levels in kidney cortex of WT, α1KI, and α1KI-CD89Tg mice as detected by quantitative PCR. Bars represent the mean. *, $P < 0.05$; **, $P < 0.01$; and ***, $P < 0.001$ (using the Mann-Whitney U test).

was observed when ELISA plates coated with recombinant sTfR1 were preincubated with TGase2 (Fig. 9 A), suggesting that similar to sCD89, TGase2 may be involved in the binding and stabilization of mesangial IgA1 deposits. This was confirmed on HMCs where binding of IgA1 was increased when cells were preincubated with TGase2 (Fig. 9 B). To evaluate the involvement of TGase2 in IgA1 deposit formation in IgAN, TGase2-deficient mice were backcrossed with α1KI-CD89Tg mice, and the development of IgAN was assessed. Immunohistochemistry analysis showed that IgA1 deposits were almost abolished in the mesangium of α1KI-CD89Tg-TGase2$^{-/-}$ mice (Fig. 9 C). Mesangial expression of TfR1 was also markedly reduced in these mice together with a decrease in MBL and C3 deposits and in macrophage infiltration (Fig. 9 D). Hematuria was abolished to the spontaneous level observed in WT animals (Fig. 9 E), which was associated with a slight decrease in proteinuria and serum creatinine levels although not reaching statistical significance (not depicted). These results indicate that sCD89 up-regulates TGase2 expression on mesangial cells and that TGase2 binds to TfR1 and IgA1 independently of a given antibody activity enhancing the formation of mesangial IgA1 deposits and the triggering of an overt IgAN.

DISCUSSION

The present study identifies new players, molecular connections, and sequences of events involved in the development of IgAN. Our data demonstrate that besides IgA1, TfR1 can also

α1KI mice (Fig. 8 B). Moreover, only α1KI-CD89Tg mice exhibited stronger colocalization in their mesangium between fibronectin and TGase2 molecules or IgA1 deposits than α1KI mice (Fig. 8, C and D), suggesting that TGase2 both controls mesangial IgA1 deposition and could contribute to the mesangial extracellular matrix expansion observed in IgAN. As TGase2 is known to be tightly involved in the stabilization of extracellular matrix (Lorand and Graham, 2003) and is colocalized with mesangial IgA1 deposits, we postulated that TGase2 could also be involved in IgA1 deposit stabilization in the mesangium. We therefore examined the in vitro interaction between TGase2 and TfR1. TGase2 strongly interacted with recombinant sTfR1 but not with an irrelevant recombinant protein, β-synuclein (Fig. 8 E). Direct TGase2–TfR1 interaction was demonstrated in pull–down assays using histidine-tagged sTfR1 as bait where TGase2 was retained and detected on Western blot (Fig. 8 F). In contrast, in the absence of sTfR1, TGase2 was not retained (Fig. 8 F). This interaction was also shown on HMCs in which binding of TGase2 was partially inhibited by recombinant sTfR1 (Fig. 8 G). We next examined whether TGase2 could amplify IgA1 binding to TfR1. Enhanced IgA1 binding to TfR1

Transglutaminase is crucial for IgA nephropathy | Berthelot et al.

interact with sCD89 and TGase2. Based on the present and previous data, we propose a model whereby polymeric IgA1 (because of abnormal glycosylation in humans or to physiological polymerization in mice) induces shedding of membrane CD89 (Grossetête et al., 1998; Launay et al., 2000) with the formation of circulating complexes containing sCD89 and IgA1. These complexes have the capacity to bind mesangial TfR1 through the ability of both sCD89 and IgA1 (Moura et al., 2001) to interact with this receptor. Upon deposition on mesangial cells, sCD89, and thus IgA1–sCD89 complexes, induces surface expression of TGase2. The latter can bind TfR1 and control its cell surface expression, allowing binding of additional IgA1–sCD89 complexes enhancing mesangial deposition. The multimolecular complexes thus stabilized on mesangial cell surface that include TfR1, TGase2, sCD89, and IgA1 would induce chronic stimulation of the cells with release of proinflammatory mediators leading to kidney disease. The tissue TGase2, which thus appears as a new partner of mesangial TfR1, is proposed to be an essential molecular actor in IgAN pathogenesis in mice as it controls mesangial deposition of IgA1 complexes that lead to renal dysfunction. TGase2 would be the factor responsible for TfR1 overexpression in primary cells implicated in IgA–related diseases (i.e., IgAN [Haddad et al., 2003] and celiac disease [Matysiak-Budnik et al., 2008]) in the absence of alterations of iron metabolism.

Since our first description of the putative role of sCD89 in generating mouse IgA deposits in the mesangium (Launay et al., 2000), there was a lack of formal demonstration that sCD89 actively participates in IgA1 mesangial deposition in mice and humans. The production of mice expressing both human IgA1 and human CD89 on monocytes/macrophages allowed us to readdress this question and to demonstrate that sCD89 is required for pathogenic mesangial IgA1 deposits leading to disease development. Interestingly, in the absence of CD89, IgA1 deposition occurring in α1KI mouse glomeruli did not lead to any detectable renal dysfunction, which is in line with observations in humans that not all subjects with IgA glomerulus deposition express overt signs of glomerulonephritis (Varis et al., 1993; Glassock, 2011). The spontaneous sCD89 production observed in mice that express human IgA1 and CD89 may be related to the high polymeric/monomeric ratio of IgA in the mouse. Indeed, although ∼30% of circulating chimeric IgA1 (composed by a human α1 heavy chain and mouse λ and κ chains) were polymeric in both α1KI and α1KI-CD89Tg mice, in human normal serum, this form represents ∼10% of total IgA (Mestecky, 1988; Kerr, 1990). Thus, small IgA1 complexes, mimicking complexes formed by underglycosylated IgA1 found in patients, may induce CD89 aggregation and shedding from myeloid cells in α1KI-CD89Tg mice as reported for human myeloid cells (Launay et al., 2000). This would result in the formation of circulating complexes containing IgA1 and sCD89 that would deposit in kidney mesangium. However, so far, there was no published evidence for mesangial sCD89 deposition in patients. Using a new polyclonal antibody raised against sCD89, we clearly detected CD89 in the mesangium of α1KI-CD89Tg mice and of IgAN patients. Acid elution procedure, a standard method to isolate antibodies and complexes from glomeruli (Woodroffe and Wilson, 1977), confirmed the presence of sCD89 in mesangial IgA1 deposits, further suggesting that the molecular mass of IgA1 complexes is a major factor promoting IgAN. In line with this observation, acidic elution of
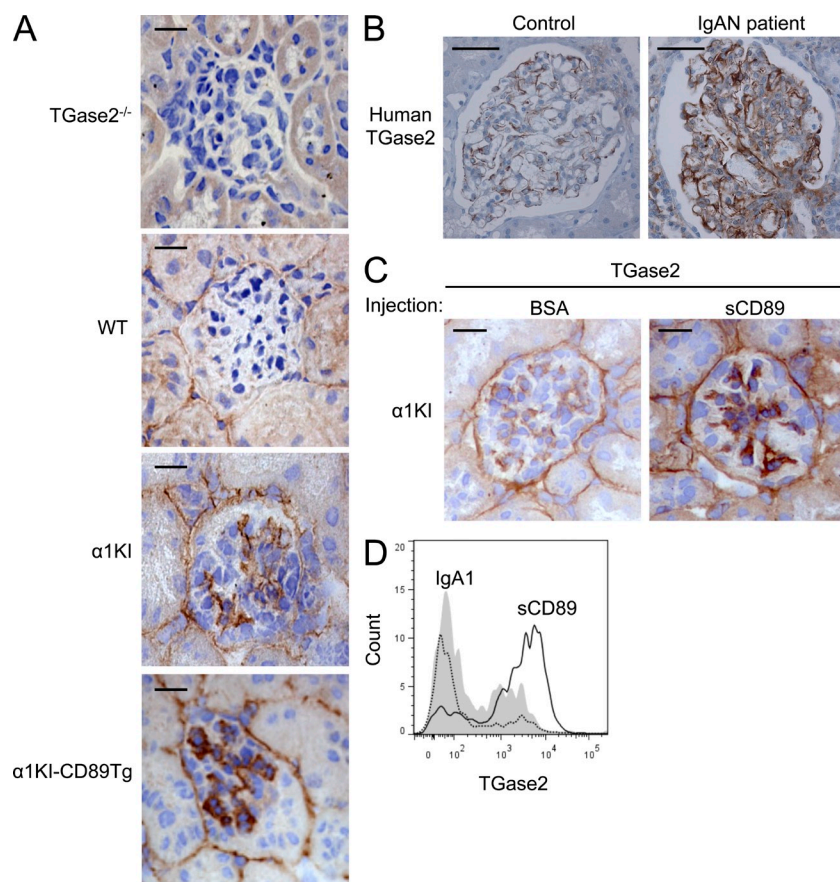

Figure 7. sCD89 induces TGase2 expression on mesangial cells. (A) TGase2 immunostaining of frozen kidney sections from TGase2$^{-/-}$, WT, α1KI, and α1KI-CD89Tg mice using a polyclonal anti-TGase2 antibody. (B) Detection of TGase2 expression by immunohistochemical analysis in kidney biopsies from a representative IgAN patient and a control with unrelated disease. (C) Immunostaining for TGase2 in frozen kidney sections of 6-wk-old α1KI mice injected i.v. with BSA or sCD89 (200 µg/mouse). Bars: (A) 10 µm; (B) 20 µm; (C) 5 µm. (D) Flow cytometry analysis of TGase2 expression on HMCs stimulated with IgA1 (gray layer) or sCD89 (white layer). The dotted layer corresponds to the isotypic-matched control. The histogram corresponds to one representative experiment of three.
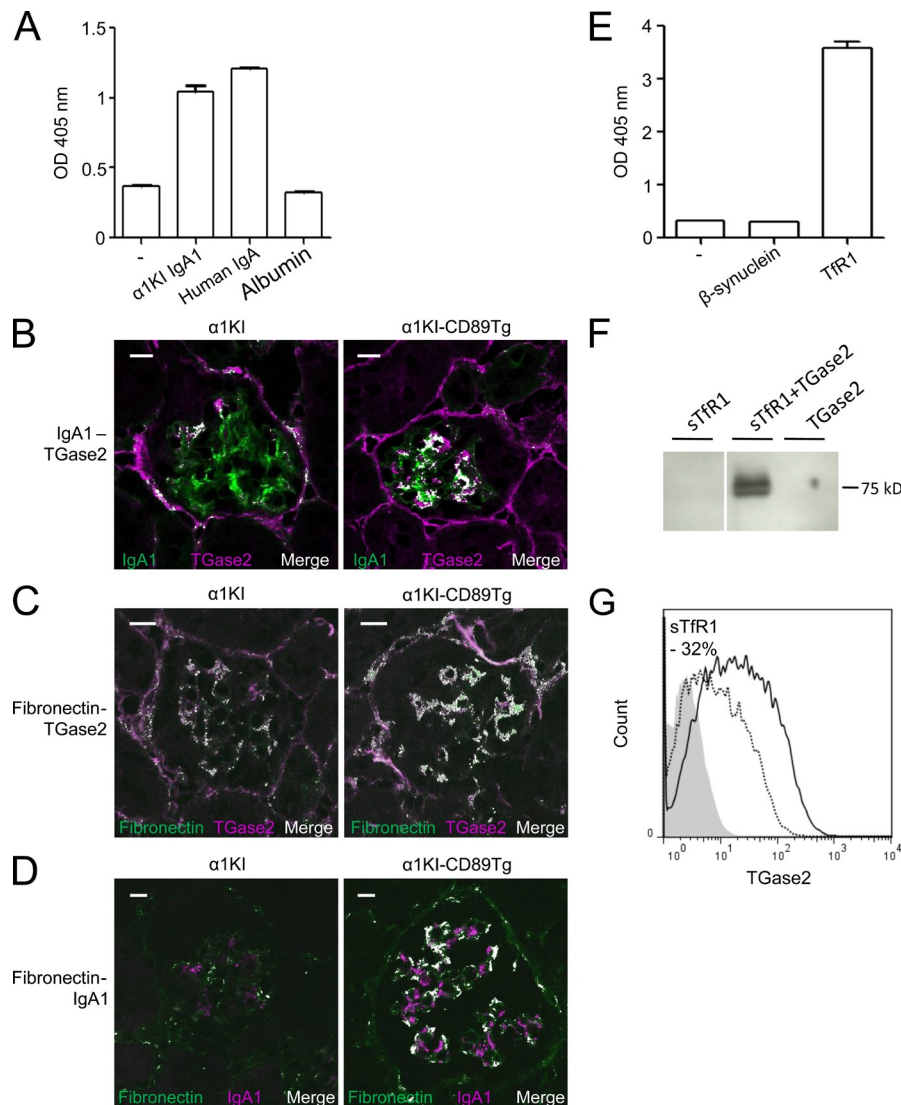
Figure 8. TGase2 interacts with TfR1 and enhances mesangial IgA1 deposition. (A) Binding of TGase2 to different types of IgA detected by ELISA using biotinylated TGase2. Albumin was used as a negative control. $n = 3$ experiments. (B–D) Double immunofluorescence for human IgA and TGase2 (B), fibronectin and TGase2 (labeled with anti–rabbit Alexa Fluor 568; C), and fibronectin and human IgA1 (D) in frozen sections from α1KI and α1KI-CD89Tg mice. Bars, 10 µm. (E) Binding of TGase2 to TfR1-His detected by ELISA using biotinylated TGase2. β-Synuclein (His-tagged protein) was used as a negative control. $n = 4$ experiments. (A and E) Error bars indicate SEM. (F) TGase2 was loaded on a column of nickel beads preincubated or not with sTfR1-His. Eluates were analyzed by SDS–10% PAGE followed by Western blot using an anti-TGase2 antibody plus anti–rabbit IgG-HRP. (G) Flow cytometry histogram (one representative experiment of six) of HMCs binding TGase2 (white layer) using biotinylated-TGase2 plus streptavidin-APC. The dashed layer represents incubation with sTfR1. The gray layer corresponds to HMCs with streptavidin-APC.

and increased serum creatinine levels. Our data may support recent observations by others in which severity of renal dysfunction in IgAN patients correlates with the disappearance of IgA1–sCD89 complexes in the circulation, suggesting that this could be caused by their increased deposition in kidneys (Boyd and Barratt, 2010; Vuong et al., 2010). The large size of the deposited pathogenic aggregates observed in these mice that include IgA1, TfR1, TfR1-associated TGase2, and sCD89 and that may also include IgA1-associated MBL with their associated serine proteases (MASP; Roos et al., 2006) may explain why deposited mesangial sCD89 has escaped detection so far. Yet, the role of sCD89 in pathogenic mesangial deposits in our IgAN murine model stresses the importance of a systematic evaluation of CD89 presence in IgAN patient biopsies. Generation of adapted molecular tools, such as our new polyclonal anti-sCD89 antibody, will be important in this regard.

TfR1, a multiligand receptor, participates in several cellular functions (Lebrón et al., 1998; Radoshitzky et al., 2007; Schmidt et al., 2008). TfR1 is a receptor for IgA1 whose binding depends on the size and the glycosylation of IgA1 (Moura et al., 2004a). TfR1–IgA1 interaction plays a crucial role in physiology where polymeric IgA1 controls erythroblast proliferation and accelerates erythropoiesis recovery in anemia (Coulon et al., 2011). In pathology, cell surface overexpression of TfR1 is a major characteristic of IgAN and celiac disease (Moura et al., 2001; Haddad et al., 2003; Matysiak-Budnik et al., 2008).

IgA1–sCD89 complexes from kidney eluates was predominantly of high molecular mass, confirming previous data obtained with IgAN patients (Monteiro et al., 1985). Interestingly, sCD89 was also detected in serum as high molecular mass forms, suggesting that sCD89 could be covalently linked to IgA1. This is in agreement with previous data showing that sCD89 can be covalently linked to IgA in a polymeric form (van der Boog et al., 2002). However, although in a previous study authors found a 30-kD sCD89 protein complexed with IgA in normal human sera (van der Boog et al., 2002), we observed a 50–70-kD sCD89 form that is exclusively found in the serum of IgAN patients (Launay et al., 2000). It is noteworthy that all sCD89 found in serum in α1KI-CD89Tg mice was associated with IgA1, demonstrating that no IgA-free sCD89 may exist in the circulation. It is also remarkable that in the absence of CD89, no high molecular mass IgA1 complexes were found in the circulation of α1KI mice. These IgA1–sCD89 complexes appeared nephrotoxic because only α1KI-CD89Tg mice developed renal failure as indicated by proteinuria, hematuria,
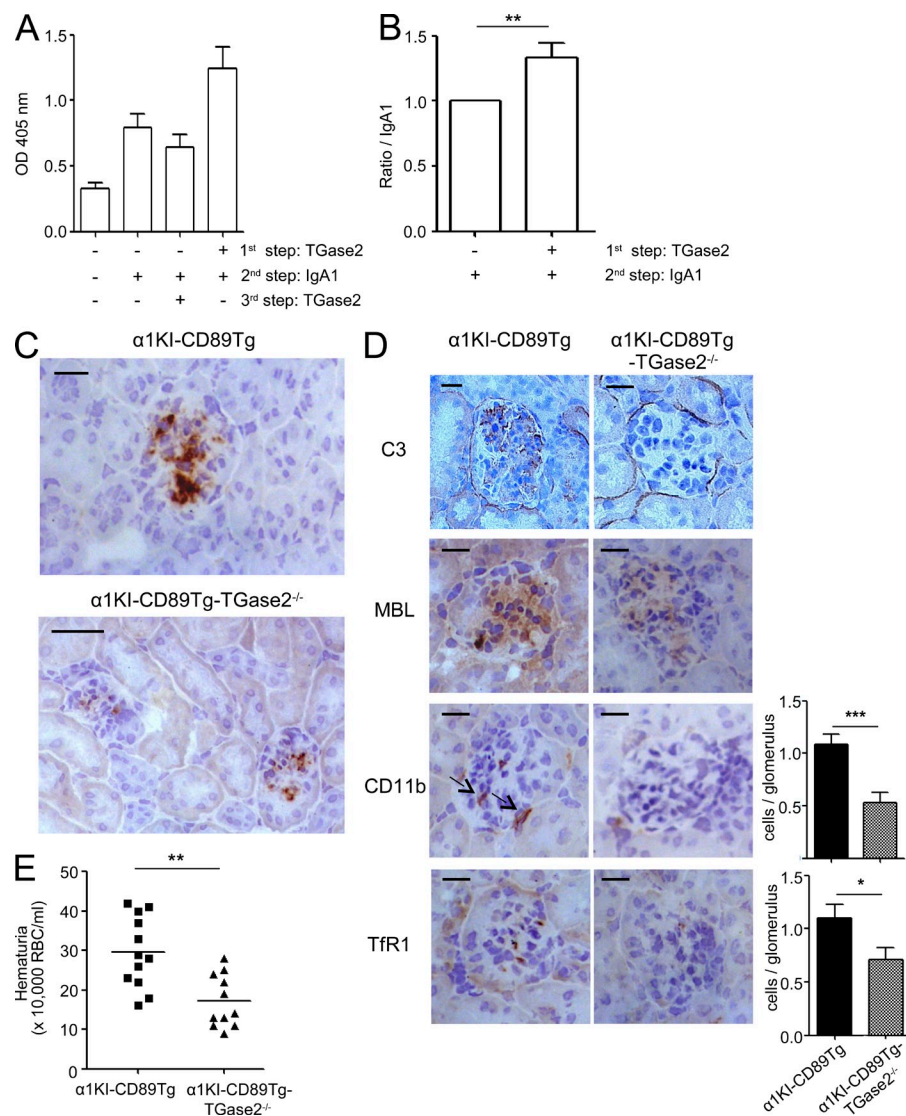
Figure 9. **TGase2–TfR1 interaction amplifies the deposition of the IgA1–sCD89 complexes and its pathological consequences.** (A and B) Binding of IgA1 on TfR1 after the addition of TGase2. (A) ELISA plates coated with sTfR1 were incubated with the indicated proteins in the order shown at 37°C and revealed with an AP-coupled polyclonal anti–human IgA antibody. $n = 3$ experiments. (B) HMCs were incubated with the different proteins in the order shown at 4°C, and binding was detected using anti–IgA-FITC. The graph shows the mean of IgA1 binding (±SEM) as a ratio of IgA1 binding mean fluorescence intensity/background mean fluorescence intensity of six independent experiments. (C and D) Immunostaining for the detection of human IgA1 deposits (C) and C3, MBL deposits, CD11b+ and TfR1+ cells (D) in frozen kidney sections from 12-wk-old α1KI-CD89Tg-TGase2−/− mice compared with α1KI-CD89Tg mice. Similar results were obtained with F4/80 mAb staining (not depicted). Arrows indicate CD11b+ cells. The graphs show the corresponding number of positive cells per glomerulus counted in 20 randomly chosen fields for each mouse at 200 magnification. $n = 3$ mice per group. Bars: (C) 10 µm; (D) 5 µm. (A, B, and D) Error bars indicate SEM. (E) Hematuria of 12-wk-old α1KI-CD89Tg and α1KI-CD89Tg-TGase2−/− mice. 12–23 mice per group. Bars represent the mean. *, $P < 0.05$; **, $P < 0.01$; and ***, $P < 0.001$ (using the Mann-Whitney U test).

However, molecular mechanisms involved in TfR1 over-expression in primary cells are not yet identified. Several factors have been shown to up-regulate TfR1 expression, including iron deprivation and human hemochromatosis protein, as well as polymeric IgA1 from patients with IgAN (Moura et al., 2005). In this study, we show that sCD89 is a new ligand for TfR1 able to up-regulate its expression on mesangial cells and induce secretion of proinflammatory cytokines such as IL-8, IL-6, and TNF. sCD89–TfR1 interaction has a marked effect on cell stimulation, suggesting that IgA1–sCD89 complexes might be responsible for a local mesangial cell activation and the development of IgAN.

Our study demonstrates that sCD89 plays a pivotal role in IgAN in mice by (a) the formation of IgA1 circulating complexes allowing their deposition in mesangium, (b) the induction of increased mesangial expression of TfR1, and (c) the induction of surface expression of TGase2. TGase2, a calcium-dependent multifunctional protein, is ubiquitously expressed in almost all cells and tissues (Lorand and Graham, 2003).

It acts predominantly as a cytosolic enzyme but can be externalized from cells by an unknown secretory pathway, after which it cross-links proteins of the extracellular matrix and induces renal fibrosis development (Fesus and Piacentini, 2002; Shweke et al., 2008). Our data reveal that TGase2 surface expression is induced by sCD89 and is up-regulated in the mesangium of α1KI-CD89Tg mice and in IgAN patients. The latter observation is in agreement with data reported by others showing increased mesangial TGase2 expression in IgAN patients (Ikee et al., 2007). Moreover, the correlation of TGase2 mesangial expression with deterioration of renal function (Ikee et al., 2007) supports our observations that only α1KI-CD89Tg mice that overexpress TGase2 develop proteinuria, whereas α1KI mice alone show no proteinuria and mild TGase2 overexpression, further suggesting that TGase2 controls the triggering of IgAN pathology. The mechanism by which TGase2 surface expression increases in turn surface expression of TfR1 remains unresolved whether it involves increased TfR1 gene transcription or interference in TfR1 cycle by favoring its recycling to, and stabilization at, the plasma membrane. Mesangial fibronectin expression is also up-regulated in α1KI-CD89Tg mice

and colocalizes with TGase2 and IgA1. Interestingly, it has been shown that TGase2 binds to fibronectin and acts as an integrin coreceptor (Lorand and Graham, 2003), emphasizing that TGase2 could intervene at multiple levels in mesangial cell activation for inflammation and fibrosis in IgAN.

In conclusion, our study demonstrates that IgA1–sCD89 complexes could initiate a process of autoamplification involving hyperexpression of TfR1 and TGase2, allowing increased mesangial deposition of pathogenic IgA1 complexes and chronic mesangial cell activation. The critical role played by TGase2 revealed by our humanized mouse model opens new perspectives for pharmacological modulation of excessive TGase2 expression as a promising strategy for therapeutic intervention in IgAN.

MATERIALS AND METHODS

Subjects. Sera were obtained from 15 patients with biopsy-proven IgAN and no steroid treatment and from 25 healthy controls with their informed consent as requested for approval by the hospital ethical committee. Renal biopsy specimens from three patients with IgAN and two with minimal change disease were studied.

Mouse procedures. α1KI mice (Duchez et al., 2010), expressing the human IgA1, were backcrossed for 15 generations with C57BL/6 CD89Tg mice expressing the WT human CD89 on monocytes/macrophages (Launay et al., 2000). Mice on 129S2/SvPasCrl-C57BL/6J mixed background were used as WT controls to α1KI, CD89Tg, and α1KI-CD89Tg mice. TGase2$^{-/-}$ C57BL/6 mice generated as described previously (De Laurenzi and Melino, 2001) were provided by G. Melino (University of Rome Tor Vergata, Rome, Italy) and P.-L. Tharaux (Institut National de la Santé et de la Recherche Médicale Unité 970, Paris, France) and were backcrossed with α1KI-CD89Tg mice. All strains were raised and maintained at the mouse facilities of the Claude Bernard Institute. All experiments were performed in accordance with the national ethical guidelines and with the approval of local authorities of the Comité d'Éthique Expérimentation Animale Bichat-Debré. Serum and kidneys were collected from 3-, 6-, 12-, 24-, and 40-wk–old male mice. 200 µg sCD89 was injected i.v. on days 0, 3, and 6 in α1KI or NOD.C.B.-17-*Prkde^{acid}*/J mice (6 wk old), and the mice were sacrificed on day 7.

Production of soluble proteins and antibodies. sCD89 and human sTfR1 were expressed and produced in lytic baculovirus/insect cell expression systems (Lebrón et al., 1998). The murine IgG1 anti-CD89 mAb A3 was produced and purified in our laboratory. The polyclonal anti-CD89 antibody was produced after injection of sCD89 in a rabbit and purified on a DEAE-Trisacryl column (BioSepra; Pall).

Histology, immunohistochemistry, and immunofluorescence. Paraffin-embedded kidney sections 4 µm in thickness were stained with PAS for morphological analysis. For immunohistochemistry, frozen kidney sections were incubated with biotinylated antibodies against human IgA, mouse IgA, mouse CD11b, mouse F4/80, human sCD89, and mouse TfR1 (BD) or with primary antibodies against mouse C3 (Abcam), mouse MBL (R&D Systems), and TGase2 (Thermo Fischer Scientific) for 1 h at room temperature. When necessary, the primary antibody incubation was followed by incubation with anti–rabbit IgG or anti–goat IgG (SouthernBiotech). Slides were mounted with the Eukitt mounting medium (Electron Microscopy Sciences) and read with an upright microscope (DM2000; Leica) at 200 magnification using the IM50 software (Leica). Human TGase2 expression in paraffin-embedded tissue sections from human normal and IgAN kidney patients was performed using an anti-TGase2 polyclonal antibody from rabbit (pab0063; Covalab). For colocalization experiments, frozen kidney sections were incubated successively with each antibody for 2 h (anti-IgA FITC, anti-CD31-biotin, rabbit anti-TGase2, goat antifibronectin, and anti–IgA-biotin) followed by incubation

with streptavidin–Alexa Fluor 568 or anti–rabbit–Alexa Fluor 568 or anti–goat FITC at room temperature. Tissue sections were mounted with Vectashield (Vector Laboratories). Slides were read with a laser-scanning confocal microscope (LSM 510; Carl Zeiss) at 630 magnification (except for IgA1-CD31 and IgA1-TGase2 staining at 400 magnification) using the LSM Image Browser (Carl Zeiss). For transmission electron microscopy, kidneys were fixed with 2.5% glutaraldehyde in PBS, postfixed with 1% osmium tetroxide in PBS, dehydrated in a graduated series of ethanol dilutions, and embedded in Epoxy Resin 812. Blocks were cut using an ultramicrotome (Ultracut; Leica). Ultra-thin sections placed on 200-mesh copper were stained with 1% uranyl acetate in 50% ethanol and Reynolds lead citrate and viewed on an electron microscope (model 1010; Jeol) coupled with a camera (MegaView III; Olympus) and SiS Analysis System version 3.2 software (Olympus) at 1,800 magnification.

Elution from mouse kidney tissues. Seven frozen kidneys per group, obtained from α1KI and α1KI-CD89Tg mice perfused with 0.9% NaCl, were thawed, pooled, and cut into small pieces, suspended in PBS, and homogenized at 4°C. After centrifugation at 4,000 *g*, the pellets were washed three times in PBS and incubated in 20 ml of 0.02 M citrate buffer, pH 3.2, for 2 h at 37°C as described previously (Jacob et al., 1987). Then, the suspension was centrifuged for 30 min at 4,000 *g*. The supernatants were neutralized at pH 7, concentrated, and adjusted to 1 ml.

Kidney functional parameters. Protein, albumin, and creatinine levels were measured in urines and creatinine levels in sera of mice using the AU400 chemistry analyzer (Olympus). For hematuria, 10 µl of fresh urines were mounted on a Malassez hemocytometer, and red cells were counted.

HPLC. 300 µl of serum or 500 µg of kidney-eluted proteins diluted in PBS was resolved by gel filtration through a Superdex 200 10/30 column (GE Healthcare) connected to an HPLC AKTA-basic automated liquid chromatography system (GE Healthcare).

Immunoblot analysis. Sera or HPLC fractions were solubilized in SDS sample buffer under nonreducing conditions and subjected to electrophoresis in 6% polyacrylamide gel. Proteins were electroblotted on polyvinylidene difluoride membranes (Millipore) and subjected to Western blot analysis using a biotinylated goat anti–human IgA (SouthernBiotech) and streptavidin coupled to horseradish peroxidase (HRP). Membranes were developed by enhanced chemical luminescence treatment (GE Healthcare). For serum immunoprecipitation assays, CD89-containing complexes were immunoprecipitated for 1 h at room temperature with mAb A3 coupled to CNBr-activated Sepharose 4B beads (GE Healthcare) followed by SDS–10% PAGE at nonreducing conditions and analyzed by Western blotting using a cocktail of anti-CD89 mAbs. For TGase2 or sCD89 with sTfR1 interaction experiments, TGase2 or sCD89 was pulled down in a column prepared with nickel beads preincubated or not with histidine-tagged sTfR1 for 4 h at 4°C. Eluates were analyzed by SDS–10% PAGE followed by Western blot using an anti-TGase2 or anti-CD89 antibody plus anti–rabbit coupled with HRP.

Cells, flow cytometry, and immunofluorescence. Splenocytes and cells from blood samples from WT, α1KI, CD89Tg, and α1KI-CD89Tg mice were stained with anti–mouse CD11b-PE-Cy7 and anti–CD89-PE antibodies (BD). Primary HMCs were purchased from Lonza and cultured as described previously (Moura et al., 2004a). Binding to HMCs was analyzed by flow cytometry using a FACSCanto II (BD). HMCs were incubated with different concentrations of α1KI mouse IgA1, biotinylated TGase, or sCD89 in successive steps on ice before washings and analysis. Complexes were formed by incubation of proteins for 1 h at 37°C. BSA was used as a negative control. The interaction with TfR1 was evaluated by using sTfR1 as a specific inhibitor. For binding inhibition, proteins were incubated with sTfR1 for 1 h on ice and then incubated with cells. Binding was evaluated using FITC-labeled anti–human IgA, streptavidin-allophycocyanin (APC) or anti–human CD89 mAb (A59-PE; BD). To examine the expression of TfR1 and TGase2, quiescent HMCs were cultured with or without sCD89. After 48-h incubation, TfR1

and TGase2 expression was analyzed by flow cytometry using an anti–TfR1-PE mAb (BD) or a biotinylated anti-TGase2 polyclonal antibody (Thermo Fisher Scientific), respectively. Cytokine (IL-8, IL-6, and TNF-α) production in the HMC culture supernatants was measured using ELISA DuoSet kits (R&D Systems) at 8 or 48 h. For immunofluorescence, HMCs were cultured on 4-well permanox Lab-Tek chamber slides in complete RPMI medium (15,000 cells/well). After 24 h, HMCs were incubated for 1 h at 4°C with preformed complexes of IgA1 and recombinant sCD89 and fixed with 2% paraformaldehyde in PBS for 15 min at room temperature. Nonspecific labeling was avoided by two 10-min incubations with sodium borohydride (NaBH₄) at 1 mg/ml followed by incubation in 4% BSA for 30 min. Cells were then labeled with a rabbit polyclonal anti-CD89 in PBS for 1.67 h, anti–human IgA-FITC (SouthernBiotech) for 1.67 h, and anti–rabbit–Alexa Fluor 568 (Invitrogen) for 1 h. After washes, HMCs were then incubated with Alexa Fluor 647–conjugated wheat germ agglutinin (Invitrogen), a cell membrane marker, in HBSS for 4 min at 4°C, followed by two washes with HBSS. Slides were mounted with Vectashield (Dako) and read with a confocal microscope (TCS SP5 II; Leica).

Human transferrin receptor gene silencing. Lentiviral vectors for human TfR1 and irrelevant control miRNA were built with the BLOCK-iT Lentiviral Pol II miR RNAi Expression System (Invitrogen). DNA sequences were designed using the BLOCK-iT RNAi Designer according to the manufacturer's recommendations and synthesized (Operon MWG). DNA oligonucleotide sequences were inserted into pcDNA6.2 vectors and transferred to pLenti6/BLOCK-iT vectors by DNA recombination. To generate lentiviral stocks, 6×10^6 293T cells were transfected with 3 µg pLenti6/BLOCK-iT–miR–human fR1, along with 9 µg ViraPower (pLP1, pLP2 ,and pLP/VSVG; Invitrogen) in Opti-MEM I (Invitrogen) without antibiotics. Cells were cultured for 72 h, and culture medium was collected, centrifuged at 4°C, 3,000 rpm for 15 min, and stored at −80°C. HMCs were infected with lentivirus in RPMI (Invitrogen) and in the presence of 6 µg/ml Polybrene (Sigma-Aldrich). Cell phenotype was analyzed 48–72 h after infection.

Quantitative real-time PCR analysis. Kidneys were homogenized, and RNA was prepared using the RNeasy Plus Mini kit (QIAGEN). 700 ng RNA was reverse transcribed using a QuantiTect RT kit (QIAGEN). Resulting cDNA was used as template for quantitative PCR analysis. Primers were purchased from Eurofins and were as follows: GAPDH, 5′-ACGGCAAAT-TCAACGGCACAGTCA-3′ (sense) and 5′-TGGGGGCATCGGCAG-AAGG-3′ (antisense); MIP-2, 5′-GCTTGAGTGTGACGCCCCCA-3′ (sense) and 5′-CAGCAGCCCAGGCTCCTCCT-3′ (antisense); IL-6, 5′-CCACG-GCCTTCCCTACTTCA-3′ (sense) and 5′-GCCATTGCACAACTCTTT-TCTCAT-3′ (antisense); and TNF, 5′-AGGCACTCCCCCAAAAGATG-3′ (sense) and 5′-TCACCCCGAAGTTCAGTAGACAGA-3′ (antisense). Gene quantification was performed in duplicate using a Chromo4 Real-Time PCR Detection System (Bio-Rad Laboratories). Data were normalized to GAPDH values.

ELISA. Plates were coated overnight with F(ab')₂ goat anti–human IgA (10 µg/well; SouthernBiotech) or A3 mAb (10 µg/well) or were directly coated with histidine-tagged TfR1 or β-synuclein or IgA1 and albumin (10 µg/well). Sera or HPLC fractions were incubated in the wells in PBS, containing 0.05% Tween, 0.1% sodium azide, and 1% BSA overnight. After washing, the anti–human IgA mAb coupled with the alkaline phosphatase (AP; BD) was added at 1:2,000 dilution for 1 h. For binding tests, biotinylated sCD89 or TGase was incubated for 2 h, and after washing, streptavidin-AP (Jackson ImmunoResearch Laboratories, Inc.) was added at 1:10,000 dilution for 30 min. The reaction was developed by adding the AP substrate (SIGMAFAST p-nitrophenyl phosphate tablets; Sigma-Aldrich).

Surface plasmon resonance assays. All the assays were performed on a Biacore X100 (GE Healthcare). The antibody A3 against CD89 was immobilized on two flow cells of a CM5 carboxymethylated dextran biosensor chip (GE Healthcare) using carbodiimide chemistry. After capture of sCD89 on one flow cell, the different purified IgAs, mouse IgA (myeloma IgA; MP

Biomedicals), human IgA1 (purified from healthy control serum using jacalin), and α1KI mouse IgA1 (myeloma IgA1, purified using DEAE column), were injected for 2 min on the two flow cells. The association and dissociation profiles were double-referenced (i.e., both the signal from the reference surface with A3 alone and from blank buffer injections were subtracted) and analyzed using the BIAevaluation software.

Statistical analysis. Nonparametric Mann-Whitney tests were performed for the different comparisons between different groups of mice and between healthy controls and IgAN patients. A p-value of <0.05 was considered significant.

REFERENCES

Berger, J., H. Yaneva, B. Nabarra, and C. Barbanel. 1975. Recurrence of mesangial deposition of IgA after renal transplantation. *Kidney Int.* 7:232–241. http://dx.doi.org/10.1038/ki.1975.35

Boyd, J.K., and J. Barratt. 2010. Immune complex formation in IgA nephropathy: CD89 a 'saint' or a 'sinner'? *Kidney Int.* 78:1211–1213. http://dx.doi.org/10.1038/ki.2010.365

Coulon, S., M. Dussiot, D. Grapton, T.T. Maciel, P.H. Wang, C. Callens, M.K. Tiwari, S. Agarwal, A. Fricot, J. Vandekerckhove, et al. 2011. Polymeric IgA1 controls erythroblast proliferation and accelerates erythropoiesis recovery in anemia. *Nat. Med.* 17:1456–1465. http://dx.doi.org/10.1038/nm.2462

De Laurenzi, V., and G. Melino. 2001. Gene disruption of tissue transglutaminase. *Mol. Cell. Biol.* 21:148–155. http://dx.doi.org/10.1128/MCB.21.1.148-155.2001

Donadio, J.V., and J.P. Grande. 2002. IgA nephropathy. *N. Engl. J. Med.* 347:738–748. http://dx.doi.org/10.1056/NEJMra020109

Duchez, S., R. Amin, N. Cogné, L. Delpy, C. Sirac, V. Pascal, B. Corthésy, and M. Cogné. 2010. Premature replacement of mu with alpha immunoglobulin chains impairs lymphopoiesis and mucosal homing but promotes plasma cell maturation. *Proc. Natl. Acad. Sci. USA.* 107:3064–3069. http://dx.doi.org/10.1073/pnas.0912393107

Fesus, L., and M. Piacentini. 2002. Transglutaminase 2: an enigmatic enzyme with diverse functions. *Trends Biochem. Sci.* 27:534–539. http://dx.doi.org/10.1016/S0968-0004(02)02182-5

Ganz, T. 2008. Iron homeostasis: fitting the puzzle pieces together. *Cell Metab.* 7:288–290. http://dx.doi.org/10.1016/j.cmet.2008.03.008

Glassock, R.J. 2011. The pathogenesis of IgA nephropathy. *Curr. Opin. Nephrol. Hypertens.* 20:153–160. http://dx.doi.org/10.1097/MNH.0b013e3283436f5c

Grossetête, B., P. Launay, A. Lehuen, P. Jungers, J.F. Bach, and R.C. Monteiro. 1998. Down-regulation of Fc alpha receptors on blood cells of IgA nephropathy patients: evidence for a negative regulatory role of serum IgA. *Kidney Int.* 53:1321–1335. http://dx.doi.org/10.1046/j.1523-1755.1998.00885.x

Haddad, E., I.C. Moura, M. Arcos-Fajardo, M.A. Macher, V. Baudouin, C. Alberti, C. Loirat, R.C. Monteiro, and M. Peuchmaur. 2003. Enhanced expression of the CD71 mesangial IgA1 receptor in Berger disease and Henoch-Schönlein nephritis: association between CD71 expression and IgA deposits. *J. Am. Soc. Nephrol.* 14:327–337. http://dx.doi.org/10.1097/01.ASN.0000046961.04917.83

Ikee, R., S. Kobayashi, N. Hemmi, T. Saigusa, T. Namikoshi, M. Yamada, T. Imakiire, Y. Kikuchi, S. Suzuki, and S. Miura. 2007. Involvement

of transglutaminase-2 in pathological changes in renal disease. *Nephron Clin. Pract.* 105:c139–c146. http://dx.doi.org/10.1159/000098646

Jacob, L., M.A. Lety, R.C. Monteiro, F. Jacob, J.F. Bach, and D. Louvard. 1987. Altered cell-surface protein(s), crossreactive with DNA, on spleen cells of autoimmune lupic mice. *Proc. Natl. Acad. Sci. USA.* 84:1361–1363. http://dx.doi.org/10.1073/pnas.84.5.1361

Kerr, M.A. 1990. The structure and function of human IgA. *Biochem. J.* 271:285–296.

Launay, P., B. Grossetête, M. Arcos-Fajardo, E. Gaudin, S.P. Torres, L. Beaudoin, N. Patey-Mariaud de Serre, A. Lehuen, and R.C. Monteiro. 2000. Fcα receptor (CD89) mediates the development of immunoglobulin A (IgA) nephropathy (Berger's disease). Evidence for pathogenic soluble receptor–Iga complexes in patients and CD89 transgenic mice. *J. Exp. Med.* 191:1999–2009. http://dx.doi.org/10.1084/jem.191.11.1999

Lebrón, J.A., M.J. Bennett, D.E. Vaughn, A.J. Chirino, P.M. Snow, G.A. Mintier, J.N. Feder, and P.J. Bjorkman. 1998. Crystal structure of the hemochromatosis protein HFE and characterization of its interaction with transferrin receptor. *Cell.* 93:111–123. http://dx.doi.org/10.1016/S0092-8674(00)81151-4

Lorand, L., and R.M. Graham. 2003. Transglutaminases: crosslinking enzymes with pleiotropic functions. *Nat. Rev. Mol. Cell Biol.* 4:140–156. http://dx.doi.org/10.1038/nrm1014

Matysiak-Budnik, T., I.C. Moura, M. Arcos-Fajardo, C. Lebreton, S. Ménard, C. Candalh, K. Ben-Khalifa, C. Dugave, H. Tamouza, G. van Niel, et al. 2008. Secretory IgA mediates retrotranscytosis of intact gliadin peptides via the transferrin receptor in celiac disease. *J. Exp. Med.* 205:143–154. http://dx.doi.org/10.1084/jem.20071204

Mestecky, J. 1988. Immunobiology of IgA. *Am. J. Kidney Dis.* 12:378–383.

Monteiro, R.C., and J.G. Van De Winkel. 2003. IgA Fc receptors. *Annu. Rev. Immunol.* 21:177–204. http://dx.doi.org/10.1146/annurev.immunol.21.120601.141011

Monteiro, R.C., L. Halbwachs-Mecarelli, M.C. Roque-Barreira, L.H. Noel, J. Berger, and P. Lesavre. 1985. Charge and size of mesangial IgA in IgA nephropathy. *Kidney Int.* 28:666–671. http://dx.doi.org/10.1038/ki.1985.181

Monteiro, R.C., I.C. Moura, P. Launay, T. Tsuge, E. Haddad, M. Benhamou, M.D. Cooper, and M. Arcos-Fajardo. 2002. Pathogenic significance of IgA receptor interactions in IgA nephropathy. *Trends Mol. Med.* 8:464–468. http://dx.doi.org/10.1016/S1471-4914(02)02405-X

Moura, I.C., M.N. Centelles, M. Arcos-Fajardo, D.M. Malheiros, J.F. Collawn, M.D. Cooper, and R.C. Monteiro. 2001. Identification of the transferrin receptor as a novel immunoglobulin (Ig)A1 receptor and its enhanced expression on mesangial cells in IgA nephropathy. *J. Exp. Med.* 194:417–425. http://dx.doi.org/10.1084/jem.194.4.417

Moura, I.C., M. Arcos-Fajardo, C. Sadaka, V. Leroy, M. Benhamou, J. Novak, F. Vrtovsnik, E. Haddad, K.R. Chintalacharuvu, and R.C. Monteiro. 2004a. Glycosylation and size of IgA1 are essential for interaction with mesangial transferrin receptor in IgA nephropathy. *J. Am. Soc. Nephrol.* 15:622–634. http://dx.doi.org/10.1097/01.ASN.0000115401.07980.0C

Moura, I.C., Y. Lepelletier, B. Arnulf, P. England, C. Baude, C. Beaumont, A. Bazarbachi, M. Benhamou, R.C. Monteiro, and O. Hermine. 2004b. A neutralizing monoclonal antibody (mAb A24) directed against the transferrin receptor induces apoptosis of tumor T lymphocytes from ATL patients. *Blood.* 103:1838–1845. http://dx.doi.org/10.1182/blood-2003-07-2440

Moura, I.C., M. Arcos-Fajardo, A. Gdoura, V. Leroy, C. Sadaka, N. Mahlaoui, Y. Lepelletier, F. Vrtovsnik, E. Haddad, M. Benhamou, and R.C. Monteiro. 2005. Engagement of transferrin receptor by polymeric IgA1: evidence for a positive feedback loop involving increased receptor expression and mesangial cell proliferation in IgA nephropathy. *J. Am. Soc. Nephrol.* 16:2667–2676. http://dx.doi.org/10.1681/ASN.2004111006

Novak, J., B.A. Julian, M. Tomana, and J. Mestecky. 2008. IgA glycosylation and IgA immune complexes in the pathogenesis of IgA nephropathy. *Semin. Nephrol.* 28:78–87. http://dx.doi.org/10.1016/j.semnephrol.2007.10.009

Pleass, R.J., J.I. Dunlop, C.M. Anderson, and J.M. Woof. 1999. Identification of residues in the CH2/CH3 domain interface of IgA essential for interaction with the human fcalpha receptor (FcalphaR) CD89. *J. Biol. Chem.* 274:23508–23514. http://dx.doi.org/10.1074/jbc.274.33.23508

Ponticelli, C., and R.J. Glassock. 2010. Posttransplant recurrence of primary glomerulonephritis. *Clin. J. Am. Soc. Nephrol.* 5:2363–2372. http://dx.doi.org/10.2215/CJN.06720810

Radoshitzky, S.R., J. Abraham, C.F. Spiropoulou, J.H. Kuhn, D. Nguyen, W. Li, J. Nagel, P.J. Schmidt, J.H. Nunberg, N.C. Andrews, et al. 2007. Transferrin receptor 1 is a cellular receptor for New World haemorrhagic fever arenaviruses. *Nature.* 446:92–96. http://dx.doi.org/10.1038/nature05539

Roos, A., M.P. Rastaldi, N. Calvaresi, B.D. Oortwijn, N. Schlagwein, D.J. van Gijlswijk-Janssen, G.L. Stahl, M. Matsushita, T. Fujita, C. van Kooten, and M.R. Daha. 2006. Glomerular activation of the lectin pathway of complement in IgA nephropathy is associated with more severe renal disease. *J. Am. Soc. Nephrol.* 17:1724–1734. http://dx.doi.org/10.1681/ASN.2005090923

Schmidt, P.J., P.T. Toran, A.M. Giannetti, P.J. Bjorkman, and N.C. Andrews. 2008. The transferrin receptor modulates Hfe-dependent regulation of hepcidin expression. *Cell Metab.* 7:205–214. http://dx.doi.org/10.1016/j.cmet.2007.11.016

Shweke, N., N. Boulos, C. Jouanneau, S. Vandermeersch, G. Melino, J.C. Dussaule, C. Chatziantoniou, P. Ronco, and J.J. Boffa. 2008. Tissue transglutaminase contributes to interstitial renal fibrosis by favoring accumulation of fibrillar collagen through TGF-beta activation and cell infiltration. *Am. J. Pathol.* 173:631–642. http://dx.doi.org/10.2353/ajpath.2008.080025

Suzuki, H., R. Fan, Z. Zhang, R. Brown, S. Hall, B.A. Julian, W.W. Chatham, Y. Suzuki, R.J. Wyatt, Z. Moldoveanu, et al. 2009. Aberrantly glycosylated IgA1 in IgA nephropathy patients is recognized by IgG antibodies with restricted heterogeneity. *J. Clin. Invest.* 119:1668–1677.

Tissandié, E., W. Morelle, L. Berthelot, F. Vrtovsnik, E. Daugas, F. Walker, D. Lebrec, J.M. Trawalé, C. Francoz, F. Durand, et al. 2011. Both IgA nephropathy and alcoholic cirrhosis feature abnormally glycosylated IgA1 and soluble CD89-IgA and IgG-IgA complexes: common mechanisms for distinct diseases. *Kidney Int.* 80:1352–1363. http://dx.doi.org/10.1038/ki.2011.276

Tomana, M., J. Novak, B.A. Julian, K. Matousovic, K. Konecny, and J. Mestecky. 1999. Circulating immune complexes in IgA nephropathy consist of IgA1 with galactose-deficient hinge region and antiglycan antibodies. *J. Clin. Invest.* 104:73–81. http://dx.doi.org/10.1172/JCI5535

van der Boog, P.J., G. van Zandbergen, J.W. de Fijter, N. Klar-Mohamad, A. van Seggelen, P. Brandtzaeg, M.R. Daha, and C. van Kooten. 2002. Fc alpha RI/CD89 circulates in human serum covalently linked to IgA in a polymeric state. *J. Immunol.* 168:1252–1258.

van der Boog, P.J., C. van Kooten, G. van Zandbergen, N. Klar-Mohamad, B. Oortwijn, N.A. Bos, A. van Remoortere, C.H. Hokke, J.W. de Fijter, and M.R. Daha. 2004. Injection of recombinant FcalphaRI/CD89 in mice does not induce mesangial IgA deposition. *Nephrol. Dial. Transplant.* 19:2729–2736. http://dx.doi.org/10.1093/ndt/gfh459

Varis, J., I. Rantala, A. Pasternack, H. Oksa, M. Jäntti, E.S. Paunu, and R. Pirhonen. 1993. Immunoglobulin and complement deposition in glomeruli of 756 subjects who had committed suicide or met with a violent death. *J. Clin. Pathol.* 46:607–610. http://dx.doi.org/10.1136/jcp.46.7.607

Vuong, M.T., M. Hahn-Zoric, S. Lundberg, I. Gunnarsson, C. van Kooten, L. Wramner, M. Seddighzadeh, A. Fernström, L.A. Hanson, L.T. Do, et al. 2010. Association of soluble CD89 levels with disease progression but not susceptibility in IgA nephropathy. *Kidney Int.* 78:1281–1287. http://dx.doi.org/10.1038/ki.2010.314

Woodroffe, A.J., and C.B. Wilson. 1977. An evaluation of elution techniques in the study of immune complex glomerulonephritis. *J. Immunol.* 118:1788–1794.

Zhang, W., B. Bi, R.G. Oldroyd, and P.J. Lachmann. 2000. Neutrophil lactoferrin release induced by IgA immune complexes differed from that induced by cross-linking of fcalpha receptors (FcalphaR) with a monoclonal antibody, MIP8a. *Clin. Exp. Immunol.* 121:106–111. http://dx.doi.org/10.1046/j.1365-2249.2000.01254.x